Proceedings of the 2005 IEEE
International Conference on Robotics and Automation
Barcelona, Spain, April 2005

Dynamic Ambiguities in Frictional Rigid-body Systems with Application to Climbing via Bracing

Aaron Greenfield, Alfred A. Rizzi and Howie Choset
Robotics Institute
Carnegie Mellon University
Pittsburgh, PA 15213 USA

***Abstract*— Constructing climbing behaviors for hyper-redundant robots that account for the system dynamics requires a model of robot dynamics under contact and friction. One common model, rigid-body dynamics with coulomb friction, unfortunately is both an ambiguous and inconsistent set of dynamic axioms. This paper addresses the ambiguity problem by developing an algorithm which computes the set of joint torques such that all solutions are guaranteed to produce the desired system behavior. This algorithm is applied to a type of robot climbing which we denote *climbing via bracing* where a hyper-redundant robot stabilizes itself against gravity by pressing outward to induce friction. By bracing with a fraction of the robot, which we term a *brace* the remainder of the robot remains free to move upward and brace at a higher location. A sequence of braces thus moves the robot upward.**

***Index Terms*— Rigid-Body Dynamics, Climbing, Hyper-redundant robot**

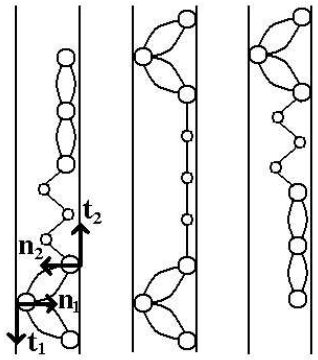

Fig. 1. Hyper-redundant robot climbing by bracing

I. Introduction

The development of climbing control algorithms for hyper-redundant snake robots which account for the dynamics of the robot is a challenging problem due to difficulties in contact modelling. In this paper, we develop an algorithm for analyzing the behavior of articulated bodies undergoing dynamic motion while in contact with the environment. The algorithm characterizes the set of joint torques that instantaneously achieve some desired system behavior.

Specifically, we consider planar rigid-body systems in a gravity field subject to point contact with coulomb friction as a contact model. A key feature of dynamics under these assumptions is that multiple dynamic solutions or no dynamic solutions are possible in different scenarios [3], [5], [6], [9], [10]. In order to form guarantees about system behavior, we seek to find behavioral policies that result in only the desired behavior. The technique developed in this paper characterizes the set of joint torques for which this guarantee can be made for an arbitrary articulated body undergoing dynamic motion.

Given this set of torques, we use it to specify dynamic behavior in a type of climbing which we term *climbing via bracing*. In climbing via bracing the robot stabilizing itself against gravity by pushing outward in order to induce friction. In our approach, the robot stabilizes a section of itself, called a *brace*, against gravity. The remainder of the robot, called a *free* section, is free to move. To ensure brace stability, we partition the robot dynamics brace and free robot sections, with the dynamics of the free portion of the robot appearing as a disturbance wrench exerted on the brace. Using the developed algorithm, we ensure a robust immobilization of the brace by considering model solutions for an entire neighborhood of applied disturbance wrenches. The free portion of the robot can then safely be moved upward. By making transitions to new braces at higher elevations, the robot sequentially climbs upward.

The dynamics algorithm presented in this paper is based on the LCP (Linear Complimentarity Problem) formulation of rigid body dynamics from Pfeiffer and Glocker [9]. They focus on formulating the dynamics and methods for finding a single solution, rather than characterization of all ambiguities. Pang and Trinkle's paper [8] defines the notion of *strong stability*, which characterizes the ambiguities possible with a static contact mode. Balkom and Trinkle [1] extend this idea, although they make the assumption of negligible system velocity, address only single rigid bodies, and do not consider the ambiguities possible within a single contact mode. Both Balkom's work and ours lacks a model of impact and thus cannot rule out ambiguities due to impact.

Within the robot climbing literature, Bretl et al. [2] develops algorithms for climbing with a multi-limbed robot. The robot is reduced to a single rigid-body and equilibrium rather than dynamic analysis is used to determine immobilization. The work focuses strongly on the planning problem of sequencing a series of fixtures. The work by Or and Rimon [7] also considers climbing for a multi-limbed robot and reduces the robot to a single rigid body. This

work considers dynamic ambiguity by developing a series of equations for the center of mass locations with constant inertia consistent with each contact mode. They consider inertial and coriolis forces as a disturbance force appended to a nominal gravitational load. The work by Yim et. al. [11] considers climbing for snake-like hyper-redundant robots, similar to our target system, by developing a gait control table (GCT).

The outline of the paper is as follows. In section 2, we present the details of the dynamics model and our algorithm for characterizing the set of ambiguity free control torques which achieve a desired dynamic behavior. In section 3 we describe an application of this to climbing via bracing. In section 4 we present example usages of the analysis tool, and in the final section we conclude.

II. Computing Torques for Desired Dynamic Behavior

Our goal in this section is to generate the set of control torques, denoted $\mathcal{T}_{\mathbf{c}}{}^*$, which uniquely achieve a desired behavior for a rigid-body system subject to frictional contacts. In order to generate the torque set, we assume that we know the current state of the system, the location of all contacts between the robot and the environment, and the kinematic and dynamic parameters of the robot.

Based on these assumptions, we develop the equations of motion using a Lagrangian formulation, which have as unknowns the system accelerations and reaction forces. We show how to solve these equations subject to both contact constraints induced by the contact model as well as additional linear *task* constraints which encode properties of desired performance.

The ambiguity in the rigid-body with coulomb friction model requires us to solve for $\mathcal{T}_{\mathbf{c}}{}^*$ in two steps. We first solve for the torques consistent with the desired *contact mode* subject to additional task constraints. We call this set the *feasible* torque set. We also compute *ambiguity* sets of torques where the model also admits solutions not satisfying the desired behavior. For example, an undetermined internal stress on a rod allows the model to predict both an equilibrium and a slipping solution. The set difference of the two types of sets gives the torques where the model predicts only desired behavior.

A. System Dynamics Equations

The Lagrangian formulation of dynamics is utilized, with generalized coordinates $\mathbf{q} \in \mathbb{R}^q$ providing a local minimal representation of the system configuration when unconstrained by contact. We assume that there are k contact points and each has a local inertial coordinate frame $X_i := (\mathbf{p}_i, \mathbf{t}_i, \mathbf{n}_i)$ with origin located at $\mathbf{p}_i$, defined such that $\mathbf{n}_i$ is normal to the contact surface and outward from the environment, and $(\mathbf{t}_i, \mathbf{n}_i)$ forms a right-handed coordinate system (see Figure 1).

For a uniform treatment of contact constraints and reaction forces, we express the position of each mechanism contact point in the corresponding contact frame X_i, through the kinematic map

$$\mathbf{x} = \mathbf{h}(\mathbf{q}) \ ,$$

where we have $\mathbf{x} := (x_{\mathbf{t}_1}, x_{\mathbf{n}_1}, ..., x_{\mathbf{t}_k}, x_{\mathbf{n}_k}) \in R^{2k}$. These kinematics also yield the contact Jacobian matrix $\mathbf{J} := D_{\mathbf{q}}\mathbf{h}$ that relates velocities and accelerations of contact points to the generalized coordinates through the relations

$$\dot{\mathbf{x}} = \mathbf{J}\dot{\mathbf{q}} \quad (1)$$

$$\ddot{\mathbf{x}} = \mathbf{J}\ddot{\mathbf{q}} + \dot{\mathbf{J}}\dot{\mathbf{q}} \ . \quad (2)$$

Dynamical equations governing the motion of the system hence take the form

$$\mathbf{M}(\mathbf{q})\ddot{\mathbf{q}} + \mathbf{C}(\mathbf{q}, \dot{\mathbf{q}})\dot{\mathbf{q}} + \mathbf{g}(\mathbf{q}) = \tau + \mathbf{J}^T\mathbf{f} \ , \quad (3)$$

where $\tau \in \mathbb{R}^t$ and $\mathbf{f} = (f_{\mathbf{t}_1}, f_{\mathbf{n}_1}, ..., f_{\mathbf{t}_k}, f_{\mathbf{n}_k}) \in \mathbb{R}^{2k}$ denote control inputs and contact reaction forces respectively; the latter expressed in local contact coordinates.

B. Contact Modes and Constraints on Dynamics

The contact model utilized in this paper is a rigid-body model, along with Coulomb's law of friction. This model imposes constraints on the dynamic equations above, which can be organized into four different *contact modes* for each contact [6]: separating (S), sliding left (L) or right (R), or fixed (F). Each contact point hence has an associated mode

$$c_i \in \mathcal{M} := \{S, L, R, F\} \ .$$

Depending on the mode, a set of constraints on velocities, accelerations and reaction forces at the contact point must be satisfied. These constraints are written in contact coordinates and summarized in Tables I and II. If the contact point is separating (S), either due to velocity or acceleration, then no reaction force is allowed, otherwise a compressive normal force is possible. Given a non-separating contact point, we consider its tangential motion. If the point is sliding left (L) or right (R) with respect to its local coordinate frame, then the tangential force must be at a maximum, otherwise the point is fixed (F) and the tangential force can be anywhere in the friction cone. Throughout the rest of the paper, we denote the overall contact mode of the system as a vector of individual modes for each contact

$$\mathbf{c} := [\ c_1, ..., c_k\ ] \in \mathcal{M}^k \ .$$

In subsequent sections, we also find it useful to encode the constraints of Tables I and II in matrix form. Given an overall contact mode $\mathbf{c}$, we denote the contact Jacobian rows corresponding to contact points in each mode by $\mathbf{J}_F$, $\mathbf{J}_S$, $\mathbf{J}_L$, and $\mathbf{J}_R$ respectively. We further denote the rows in

TABLE I

Normal Force, Velocity, and Acceleration Constraints

Mode	Velocity	Acceleration	$f_{\mathbf{n}_i}$
S	$\dot{x}_{\mathbf{n}_i} > 0$	—	$f_{\mathbf{n}_i} = 0$
S	$\dot{x}_{\mathbf{n}_i} = 0$	$\ddot{x}_{\mathbf{n}_i} \geq 0$	$f_{\mathbf{n}_i} = 0$
F,L,R	$\dot{x}_{\mathbf{n}_i} = 0$	$\ddot{x}_{\mathbf{n}_i} = 0$	$f_{\mathbf{n}_i} \geq 0$

TABLE II

TANGENTIAL FORCE, VELOCITY, AND ACCELERATION CONSTRAINTS

Mode	Velocity	Acceleration	$f_{\mathbf{t}_i}$
R	$\dot{x}_{\mathbf{t}_i} > 0$	—	$f_{\mathbf{t}_i} = -\mu f_{\mathbf{n}_i}$
L	$\dot{x}_{\mathbf{t}_i} < 0$	—	$f_{\mathbf{t}_i} = \mu f_{\mathbf{n}_i}$
R	$\dot{x}_{\mathbf{t}_i} = 0$	$\ddot{x}_{\mathbf{t}_i} \geq 0$	$f_{\mathbf{t}_i} = -\mu f_{\mathbf{n}_i}$
L	$\dot{x}_{\mathbf{t}_i} = 0$	$\ddot{x}_{\mathbf{t}_i} \leq 0$	$f_{\mathbf{t}_i} = \mu f_{\mathbf{n}_i}$
F	$\dot{x}_{\mathbf{t}_i} = 0$	$\ddot{x}_{\mathbf{t}_i} = 0$	$\lvert f_{\mathbf{t}_i} \rvert \leq \mu f_{\mathbf{n}_i}$

the normal and tangential directions by subscripting with $\mathbf{n}$ or $\mathbf{t}$.

For equality constraints on system accelerations, we can then use the appropriate rows of (2) to yield

$$\begin{bmatrix} \mathbf{J}_F \\ \mathbf{J}_{L_\mathbf{n}} \\ \mathbf{J}_{R_\mathbf{n}} \end{bmatrix} \ddot{\mathbf{q}} + \begin{bmatrix} \mathbf{J}_F \\ \mathbf{J}_{L_\mathbf{n}} \\ \mathbf{J}_{R_\mathbf{n}} \end{bmatrix} \dot{\mathbf{q}} = \begin{bmatrix} 0 \\ 0 \\ 0 \end{bmatrix} . \tag{4}$$

Similarly, for equality constraints on the contact reaction forces, we have

$$\begin{bmatrix} \mathbf{0} & \mathbf{I}_{2F} & \mathbf{0} & \mathbf{0} & \mathbf{0} & \mathbf{0} \\ \mathbf{0} & \mathbf{0} & -\mu\mathbf{I}_L & \mathbf{I}_L & \mathbf{0} & \mathbf{0} \\ \mathbf{0} & \mathbf{0} & \mathbf{0} & \mathbf{0} & \mu\mathbf{I}_R & \mathbf{I}_R \end{bmatrix} \begin{bmatrix} \mathbf{f}_F \\ \mathbf{f}_S \\ \mathbf{f}_{L_\mathbf{n}} \\ \mathbf{f}_{L_\mathbf{t}} \\ \mathbf{f}_{R_\mathbf{n}} \\ \mathbf{f}_{R_\mathbf{t}} \end{bmatrix} = \mathbf{0} , \tag{5}$$

where $\mathbf{I}_F$ is the identity matrix of size equal to the number of fixed contact points, for example. The remaining inequality constraints from Tables I and II take the form

$$\begin{bmatrix} \mathbf{J}_{S_n} \\ -\mathbf{J}_{L_t} \\ \mathbf{J}_{R_t} \end{bmatrix} \ddot{\mathbf{q}} + \begin{bmatrix} \dot{\mathbf{J}}_{S_n} \\ -\dot{\mathbf{J}}_{L_t} \\ \dot{\mathbf{J}}_{R_t} \end{bmatrix} \dot{\mathbf{q}} \geq 0 , \tag{6}$$

for accelerations and

$$\begin{bmatrix} \mu\mathbf{I}_F & -\mathbf{I}_F & \mathbf{0} & \mathbf{0} & \mathbf{0} & \mathbf{0} & \mathbf{0} \\ \mu\mathbf{I}_F & \mathbf{I}_F & \mathbf{0} & \mathbf{0} & \mathbf{0} & \mathbf{0} & \mathbf{0} \\ \mathbf{0} & \mathbf{0} & \mathbf{0} & \mathbf{I}_L & \mathbf{0} & \mathbf{0} & \mathbf{0} \\ \mathbf{0} & \mathbf{0} & \mathbf{0} & \mathbf{0} & \mathbf{0} & \mathbf{I}_R & \mathbf{0} \end{bmatrix} \begin{bmatrix} \mathbf{f}_{F_n} \\ \mathbf{f}_{F_t} \\ \mathbf{f}_S \\ \mathbf{f}_{L_n} \\ \mathbf{f}_{L_t} \\ \mathbf{f}_{R_n} \\ \mathbf{f}_{R_t} \end{bmatrix} \geq \mathbf{0} , \tag{7}$$

for contact reaction forces. Acceleration inequalities of (6) are only applicable to separating contact points with zero normal velocity and sliding contact points with zero tangential velocity as indicated in the Tables I and II.

In this paper, we also consider the possibility of imposing additional model specific linear constraints, which we term *task constraints*. Task constraints are user imposed conditions that are not physically necessary, but rather application specific, desired properties of dynamic solutions. For hyper-redundant robots, additional constraints beyond the contact mode will be necessary to specify immobilization due to the large internal degrees of freedom of the robot. Actuator saturations may also be specified as additional constraints.

Both contact and task equality constraints are merged into the linear system

$$\mathbf{A}^{\ddot{\mathbf{q}}}\, \ddot{\mathbf{q}} = \mathbf{B}^{\ddot{\mathbf{q}}}\, \tau + \mathbf{b}^{\ddot{\mathbf{q}}} \tag{8}$$

$$\mathbf{A}^{\mathbf{f}}\, \mathbf{f} = \mathbf{B}^{\mathbf{f}}\, \tau + \mathbf{b}^{\mathbf{f}} , \tag{9}$$

and all inequality constraints are merged into the system

$$\mathbf{N}^{\ddot{\mathbf{q}}}\, \ddot{\mathbf{q}} \geq \mathbf{E}^{\ddot{\mathbf{q}}}\, \tau + \mathbf{e}^{\ddot{\mathbf{q}}} \tag{10}$$

$$\mathbf{N}^{\mathbf{f}}\, \mathbf{f} \geq \mathbf{E}^{\mathbf{f}}\, \tau + \mathbf{e}^{\mathbf{f}} . \tag{11}$$

Note that in this paper we do not consider impact models, precluding us from computing solutions to the system whenever $\dot{x}_{\mathbf{n}_i} < 0$ or $\ddot{x}_{\mathbf{n}_i} < 0$. Among other ramifications, Painlevé type problems [3], [6], [10] where sliding friction would result in rigid-body penetration will thus have no solution, and ambiguities due to impacts are ignored. This limits the applicability of our methods to situations where consideration of impacts is not important.

C. Form of torque set $\mathcal{T}_\mathbf{c}^*$

As noted, the goal of this section is to compute the set $\mathcal{T}_\mathbf{c}^*$ of torques uniquely consistent with the contact mode $\mathbf{c}$ subject to additional task constraints. Due to the possibility of ambiguity, we first solve for the feasible torque set, denoted $\mathcal{T}_\mathbf{c}$. This is the polygonal set of torques which admit model solutions satisfying the equations of motion, contact constraints for mode $\mathbf{c}$, and the task constraints.

A torque in $\mathcal{T}_\mathbf{c}$ may also admit model solutions which do not satisfy desired behavior, and thus produce an ambiguity, in two ways. First, the torque may admit a solution which satisfies the equations of motion, but also the contact constraints for another mode $\bar{\mathbf{c}}$. We term this type of ambiguity an across mode ambiguity, and denote the torques consistent with this new mode by $\mathcal{T}_{\bar{\mathbf{c}}}$. Secondly, the torque may admit a solution which satisfies the equation of motion, and contact constraints for $\mathbf{c}$ but does not satisfy a task constraint. We term this type of ambiguity a within mode ambiguity and denote the torques consistent with mode $\mathbf{c}$ and the negation of the i^{th} task constraint by $\mathcal{T}_\mathbf{c}^{\bar{i}}$.

The set of torques, $\mathcal{T}_\mathbf{c}{}^*$, uniquely consistent with the desired behavior is then the set difference of the feasible set and the ambiguity sets

$$\mathcal{T}_\mathbf{c}{}^* := \mathcal{T}_\mathbf{c} - \bigcup_{\bar{\mathbf{c}} \in (\mathcal{M}^k - \mathbf{c})} (\mathcal{T}_\mathbf{c} \cap \mathcal{T}_{\bar{\mathbf{c}}}) - \bigcup_{i \in [1..j]} \left(\mathcal{T}_\mathbf{c} \cap \mathcal{T}_\mathbf{c}^{\bar{i}} \right) ,$$

with j being the number of task constraints. This is the set difference of convex polygonal sets, which will, in general, be a non-convex volume in the space of control inputs.

D. Computing Feasible Set

Given the desired mode $\mathbf{c}$ with task constraints, we compute the feasible set by first solving the corresponding system of linear equality constraints. This solution is then substituted into the corresponding system of inequality constraints, which is reduced to yield $\mathcal{T}_\mathbf{c}$.

The three types of equality constraints that must be satisfied by the model unknowns $(\ddot{\mathbf{q}}, \mathbf{f})$ are the equations of motion (3), the contact and task constraints on $\ddot{\mathbf{q}}$ (8),

and the contact and task constraints on $\mathbf{f}$ (9). We collect all equality constraints in a single linear system

$$\begin{bmatrix} \mathbf{A}^{\ddot{\mathbf{q}}} & \mathbf{0} \\ \mathbf{0} & \mathbf{A}^{\mathbf{f}} \\ \mathbf{M}(\mathbf{q}) & -\mathbf{J}^T \end{bmatrix} \begin{bmatrix} \ddot{\mathbf{q}} \\ \mathbf{f} \end{bmatrix} = \begin{bmatrix} \mathbf{B}^{\ddot{\mathbf{q}}} & \mathbf{0} \\ \mathbf{0} & \mathbf{B}^{\mathbf{f}} \\ \mathbf{0} & \mathbf{I} \end{bmatrix} \tau + \begin{bmatrix} \mathbf{b}^{\ddot{\mathbf{q}}} \\ \mathbf{b}^{\mathbf{f}} \\ \mathbf{b}^{dyn} \end{bmatrix} \quad (12)$$

where $\mathbf{b}^{dyn} := -\mathbf{g}(\mathbf{q}) - \mathbf{C}(\mathbf{q}, \dot{\mathbf{q}})\dot{\mathbf{q}}$. We simplify notation and write this system as

$$\mathbf{A} \begin{bmatrix} \ddot{\mathbf{q}} \\ \mathbf{f} \end{bmatrix} = \mathbf{B}\tau + \mathbf{b}. \quad (13)$$

Different possible rank conditions of the matrix $\mathbf{A}$ result in different forms for the linear system solution. In the most degenerate case, where $\mathbf{A}$ is neither f.c.r. (full column rank) nor f.r.r. (full row rank) and the affine subspace spanned by the right-hand side of (13) does not fully lie in the column space of $\mathbf{A}$ the solution is

$$\begin{bmatrix} \ddot{\mathbf{q}} \\ \mathbf{f} \end{bmatrix} = \mathbf{A}^{\dagger}\mathbf{B}\tau + \mathbf{A}^{\dagger}\mathbf{b} + \mathbf{N}(\mathbf{A})\mathbf{w} \quad (14)$$
$$\text{s.t. } \tau = \mathbf{A}^p\tau_p + \mathbf{b}^p \ ,$$

where $\mathbf{A}^{\dagger}$ is pseudo-inverse, $\mathbf{N}(\mathbf{A})$ is a null space basis, and $\mathbf{w}$ is the parametrization of this null space. The second line is the affine subspace of torques for which the right-hand side of (13) lies in the column space of $\mathbf{A}$; the torques for which the linear system has a solution.

The solution becomes simpler when the two degeneracies are removed. When $\mathbf{A}$ is f.c.r., the null space degeneracy, and the corresponding portion of the solution $\mathbf{N}(\mathbf{A})$, are no longer present. When the affine subspace spanned by the right-hand side of (13) lies in the column space of $\mathbf{A}$, then a solution exists for all torques and the second line is eliminated. Note that the potential reduction in the actuation freedom through the smaller parametrization τ_p must be taken into account when computing the feasible set $\mathcal{T}_{\mathbf{c}}$. This can either be done by writing this set on the reduced coordinates τ_p or simply keeping track of the reduced torque subspace.

After solving the equality system of constraints, we take into account the inequality constraints in order to form the feasible set. The inequality constraints from (11) and (10) are grouped into a single system

$$\begin{bmatrix} \mathbf{N}^{\ddot{\mathbf{q}}} & \mathbf{0} & \mathbf{E}^{\ddot{\mathbf{q}}} \\ \mathbf{0} & \mathbf{N}^{\mathbf{f}} & \mathbf{E}^{\mathbf{f}} \end{bmatrix} \begin{bmatrix} \ddot{\mathbf{q}} \\ \mathbf{f} \\ \tau \end{bmatrix} \geq \begin{bmatrix} \mathbf{e}^{\ddot{\mathbf{q}}} \\ \mathbf{e}^{\mathbf{f}} \end{bmatrix}. \quad (15)$$

Using the equality constraint solution (14) to eliminate $(\ddot{\mathbf{q}}, \mathbf{f})$, the inequality system takes the form

$$\mathbf{N} \begin{bmatrix} \tau \\ \mathbf{w} \end{bmatrix} \geq \mathbf{e} \ . \quad (16)$$

The control inputs and ambiguity variables which satisfy this system correspond to dynamic solutions which satisfy all equality and inequality constraints. The projection of this set on to the τ axes is the desired feasible set $\mathcal{T}_{\mathbf{c}}$. This projection may be accomplished by a polytope projection technique such as Fourier-Motzkin [4]. The projection process often produces redundant constraints and an additional reduction through linear programming is required to produce a minimal representation.

E. Computing Ambiguity Sets

The next step of the algorithm is to determine subsets of the joint torques in $\mathcal{T}_{\mathbf{c}}$ which also admit non-desired dynamic solutions. The identification of these sets is necessary to guarantee system performance in spite of model ambiguity. We consider the two types of ambiguities: between mode and within mode.

1) Between mode ambiguities: To determine if another contact mode produces an ambiguity for some $\tau \in \mathcal{T}_{\mathbf{c}}$ we repeat the feasibility analysis of the previous section for the new contact mode $\bar{\mathbf{c}}$. However, in this case, we need not apply any additional task constraints. If the resultant intersection, denoted $\mathcal{T}_{\mathbf{c}} \cap \mathcal{T}_{\bar{\mathbf{c}}}$ is not empty, which we may test by Linear Program, then there is an ambiguity.

Instead of determining the feasibility of every possible mode $\bar{\mathbf{c}}$, we first determine whether $\bar{\mathbf{c}}$ is kinematically feasible. That is, disregarding the dynamics of the system, we determine if there exists a system acceleration achieving the contact mode. The existence of such an acceleration solution is equivalent to the consistency of the contact mode acceleration equality and inequality constraints, and can be checked via Linear Program.

2) Within mode ambiguities: It is also possible for $\tau \in \mathcal{T}_{\mathbf{c}}$ to admit model solutions which do not satisfy the task constraints. If such a solution exists, it must satisfy all contact mode constraints, but not one of the task constraints, therefore these sets are characterized by adding a single negated task constraint to the mode constraints.

Repeating the feasibility analysis for the constraint set formed by negating the i^{th} task constraint gives us the set $\mathcal{T}_{\mathbf{c}}^{\bar{i}}$ which we test as above for intersection with $\mathcal{T}_{\mathbf{c}}$.

III. Climbing via Bracing

Using the analysis tool of the previous section, we can determine control torques τ which enable climbing behaviors for hyper-redundant robots. Particularly, we look at a type of climbing, which we term *climbing via bracing*, and show how to generate the set of robust immobilizing torques for a section of the robot, which we term a *brace*. Given this immobilization, the remainder of the robot moves to a higher elevation and re-braces.

A. Climbing definitions

In order to define climbing via bracing, we first define climbing. We consider climbing a sequence of stable grasps that move the lowest robot/environment contact up or down using grasp transitions which maintain one load-bearing contact point instantaneously fixed. We further require that gravity and contact forces are the dominant external forces used for locomotion.

We identify the lowest contact point as the critical point to move as opposed to the center of mass, to rule out scenarios where the robot rests on the ground and extends itself upward. The grasps are required to be stable to rule out transitory changes in elevation. Transitions are required to maintain one load bearing contact to rule out pure sliding and a flight phase, but allow rolling or fixed contacts.

Within this framework, we distinguish climbing techniques by the method they utilize to stabilize grasps and the transition method between grasps. Climbing by bracing is then defined as climbing in which the method of stabilizing grasps is by coulomb friction induced by pressing outward against geometrically opposing environmental surfaces. This is opposed to the climbing technique proposed in [2] and [7] where the friction force is induced by gravity pressing the robot into the environment. This also distinguishes it from climbing using special structures such as adhesive contacts or penetrating spikes.

B. Dynamic reduction

One grasp transition method for climbing via bracing is to immobilize a *brace* section of the robot, reach out with the remaining *free* section, and then re-brace the robot at a different location. In order to determine brace immobilization, we consider its dynamics alone, with the remainder of the robot reduced to a disturbance force. That is, partition the coordinates of the robot into two sets q_b and q_f, where q_b are the coordinates for the brace. The dynamics of the robot can be partitioned as

$$\begin{bmatrix}\mathbf{M}_{ff}\ \mathbf{M}_{fb}\\ \mathbf{M}_{bf}\ \mathbf{M}_{bb}\end{bmatrix}\begin{bmatrix}\ddot{\mathbf{q}}_f\\ \ddot{\mathbf{q}}_b\end{bmatrix}+\begin{bmatrix}\mathbf{C}_{ff}\ \mathbf{C}_{fb}\\ \mathbf{C}_{bf}\ \mathbf{C}_{bb}\end{bmatrix}\begin{bmatrix}\dot{\mathbf{q}}_f\\ \dot{\mathbf{q}}_b\end{bmatrix}+\begin{bmatrix}\mathbf{g}_{ff}+\mathbf{g}_{fb}\\ \mathbf{g}_{bb}+\mathbf{g}_{bf}\end{bmatrix}=\begin{bmatrix}\tau_f\\ \tau_b\end{bmatrix}+\begin{bmatrix}\mathbf{J}_{ff}\ \mathbf{J}_{fb}\\ \mathbf{J}_{bf}\ \mathbf{J}_{bb}\end{bmatrix}\begin{bmatrix}\mathbf{f}_f\\ \mathbf{f}_b\end{bmatrix}.$$

Now rearranging the bottom row of the partition we have

$$\mathbf{M}_{bb}\ddot{\mathbf{q}}_b+\mathbf{C}_{bb}\dot{\mathbf{q}}_b+\mathbf{g}_{bb}=\tau_b+\tau_d+\mathbf{J}_{bb}^T\mathbf{f}_b$$

where $\tau_d=-(\mathbf{M}_{bf}\ddot{\mathbf{q}}_f+\mathbf{C}_{bf}\dot{\mathbf{q}}_f+\mathbf{g}_{bf}-\mathbf{J}_{bf}^T\mathbf{f}_f)$. That is, τ_d is a disturbance wrench exerted on the brace consisting of inertial, fictional, gravitational, and reaction force components due to motion of the free section of the robot.

C. Application of analysis tool to reduced dynamics

Given a bounded convex set of possible disturbances $D=\{\tau_d : N^d\tau_d \geq b^d\}$, our analysis tool can be used to characterize the feasible and ambiguity sets in the space of applied forces (τ_b,τ_d). In order to guarantee a robust brace immobilization, we ensure that immobilization is the only possible dynamic solution for all disturbances $\tau_d \in D$.

To do this, consider the feasible set $\mathcal{T}_\mathbf{c}$. For a particular disturbance located at a vertex of D, denoted $v=(d_1,d_2,...)$, the hyperplane constraints characterizing $\mathcal{T}_\mathbf{c}$ reduce to a new set of hyperplane constraints $\mathcal{T}_\mathbf{c}^v$ on only τ_b. This new set represents the torques for which immobilization is feasible for the disturbance v. Due to the convexity of $\mathcal{T}_\mathbf{c}$ the set $\mathcal{T}_\mathbf{c}^{'}=\cap_v C_v$, where v ranges over all vertices of D, is the set of torques for which immobilization is feasible for all disturbance forces. We now determine the ambiguous torques by projecting each ambiguity region using Fourier-Motzkin on to the τ-axes to produce another ambiguity set, denoted by $\mathcal{T}_{\bar{\mathbf{c}}}^{'}$ and $\mathcal{T}_\mathbf{c}^{\bar{i}'}$. Any joint torque which admits a non-immobilizing solution for any disturbance is represented in the projection. The set difference $\mathcal{T}_\mathbf{c}^{'}-\cup\mathcal{T}_{\bar{\mathbf{c}}}^{'}-\cup\mathcal{T}_\mathbf{c}^{\bar{i}'}$ are the torques which only admit brace immobilizing model solutions for all $\tau_d \in D$.

IV. Examples

We develop three examples of increasing complexity to illustrate the presented techniques for generating immobilizing torques. The first example looks at immobilizing a simple 2-link system between parallel walls and discusses a case where model ambiguity becomes a factor. The second example illustrates the use of additional task constraints in immobilizing a 6-link system, and the third looks at robust brace immobilization for a climbing 5-link system.

All example systems have link length $L=.127[m]$, friction coefficient $\mu=.3$, and point masses $m=.0849[kg]$ located at the end of each link, with only a single point mass m at the joints. All systems have generalized coordinates $\mathbf{q}=(x,y,\theta,\theta_1,...,\theta_n)$. Coordinates (x,y) specify the end point of link one, θ the orientation of the link, and the angles $(\theta_1,...,\theta_n)$ describe the n joint angles (See Figure 2). The velocity of each system is zero.

A. 2-Link Snake Immobilization

In this example, we find the joint torques which unambiguously immobilize $(\ddot{\mathbf{q}}=0)$ the 2-link snake shown in Figure 2 with configuration $\mathbf{q}=(0,0,135^o,-90^o)$.

We start by encoding the desired immobilization behavior as the contact mode $\mathbf{c}=(F\,F\,F)$. The mode $\mathbf{c}$ imposes the contact equality constraints $\mathbf{0}=\mathbf{J}\ddot{\mathbf{q}}$ on acceleration and the inequalities $\mu f_{n_i}\pm f_{t_i}\geq 0$ relating tangential and normal forces at each contact point. Solving these constraints, along with the Lagrange equations gives us the feasible set $\mathcal{T}_\mathbf{c}=\{\tau\leq -.19[Nm]\}$.

Solving for the torques consistent with other contact modes $\bar{\mathbf{c}}$ gives no overlap with this set, so there are no ambiguity sets and $\mathcal{T}_\mathbf{c}^*=\mathcal{T}_\mathbf{c}$, meaning all feasible torques unambiguously admit immobilizing solutions. There would be ambiguities, however, for larger coefficients of friction, where the links fall within the friction cone.

B. 6-Link Snake Immobilization

Here we consider the immobilization problem for the 6-link system shown in Figure 3 with coordinates $\mathbf{q}=(0,0,160^o,-20^o,-20^o,-60^o,-20^o,-20^o)$.

The key difference between this example and the previous is the extra system degrees of freedom which mean that the mode $\mathbf{c}=(F\,F\,F)$ does not by itself encode immobilizing behavior. To encode this behavior, we add the task constraints $\mathbf{I}\ddot{\mathbf{q}}=\mathbf{0}$, with $\mathbf{I}$ the identity matrix.

Under this assumption we find the feasible set $\mathcal{T}_\mathbf{c}$ as before, which is a three dimensional set despite the five joint torque space due to the additional task constraints.

There are ambiguities possible both within mode $\mathbf{c}$ and with other modes $\bar{\mathbf{c}}$. Solving for the ambiguity sets we find no ambiguities, so $\mathcal{T}_\mathbf{c}^*=\mathcal{T}_\mathbf{c}$. For space concerns, we do not report this set, but a single immobilizing torque from it is $(\tau_{\theta_1},\tau_{\theta_2},\tau_{\theta_3},\tau_{\theta_4},\tau_{\theta_5})=(-0.15,-0.58,-1.20,-0.70,-0.30)[Nm]$.

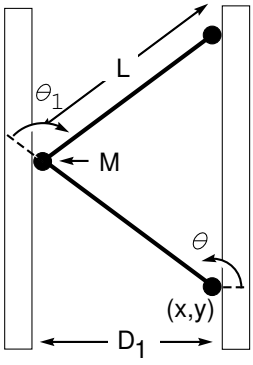

Fig. 2. 2 Link Snake braced between parallel walls

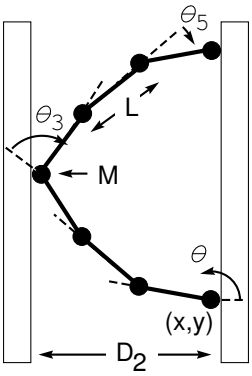

Fig. 3. 6 Link Snake braced between parallel walls

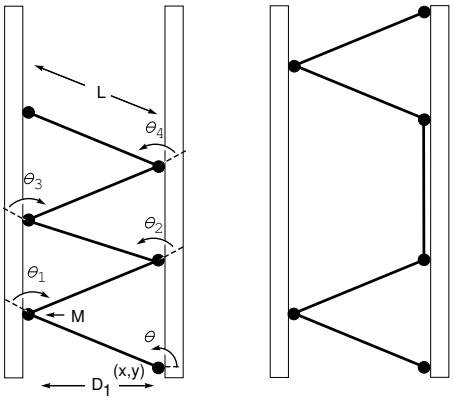

Fig. 4. 5 Link Snake climbing via bracing

C. 2-Link brace, 5-Link Snake

In the final example, we want to find the set of torques which *robustly* immobilize the 2-link brace for a range of disturbance forces D. The configuration $\mathbf{q}$ is the same as in the first example.

We start by assuming that the free portion of the snake moves in a particular trajectory between the configurations shown in Figure 4. This induces a time-dependent gravitational, inertial, and coriolis disturbance load on the brace coordinates, shown in Figure 5. We can conservatively bound this with the disturbance set $D = [-.2, .1] \times [-3.0, -2.3] \times [-.05, .25] \times [-.25, 0]$.

Now, we find the feasible set $\mathcal{T}_{\mathbf{c}}$ of joint torques and disturbance forces (τ_b, τ_d) for which the brace is immobilized. By looking at the vertices of the disturbance region, we derive from this the set $\mathcal{T}_{\mathbf{c}}^{'} = \{\tau \leq -.61[Nm]\}$, of joint torques for which immobilization is feasible regardless of the disturbance force.

The ambiguity sets are similarly calculated for other modes $\bar{\mathbf{c}}$, and projected to produce the sets $\mathcal{T}_{\bar{\mathbf{c}}}^{'}$ for which these modes are possible for some disturbance in D. In this case, we find no ambiguity, so the set of torques which robustly immobilizes the brace is $\mathcal{T}_{\bar{\mathbf{c}}}^{'}$.

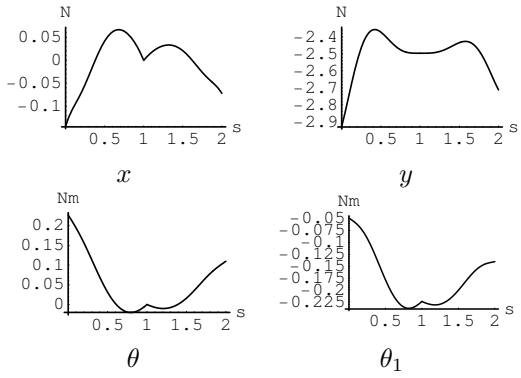

Fig. 5. Disturbance forces on brace coordinates as a function of time

V. Conclusion/Future Work

The paper presents an algorithm for characterizing force and motion ambiguities for arbitrary articulated bodies undergoing dynamic motion. This algorithm is applied to climbing via bracing. One extension to the work would be a sensitivity analysis to guarantee desired behavior for a range of system configurations or friction coefficients. Other extensions include addition of an impact model, consideration of the 3-D contact case, and theorems on when particular ambiguities are possible.

With respect to climbing via bracing, there are several higher level problems such as brace selection, foothold selection, and planning. In brace selection, we decide which robot section to immobilize. In foothold selection, we decide on brace configuration and contacts, and in the planning problem we sequence a series of braces.

Acknowledgment

The authors would like to thank Devin Balkom, Siddhartha Srinivasa, Dave Conner, and Uluc Saranli.

References

[1] D. Balkom and J.C. Trinkle. Computing wrench cones for planar rigid body contact tasks. *International Journal Of Robotics Research*, 21, 2002.

[2] T. Bretl, S. Rock, and J.C. Latombe. Motion planning for a three-limbed climbing robot in vertical natural terrain. In *Proc. IEEE Int. Conf. on Robotics and Automation*, 2003.

[3] Michael Erdmann. On a representation of friction in configuration space. *International Journal Of Robotics Research*, 13, 1994.

[4] T. Huynh, C. Lassez, and J-L. Lassez. Practical issues on the projection of polyhedral sets. *Ann. Math Artificial Intelligence*, 6:295–316, 1992.

[5] C.E. Lemke. Recent results in complementarity problems. In *Nonlinear programming*, pages 349–384. Academic Press, 1970.

[6] Matthew T. Mason. *Mechanics of Robotic Manipulation*. The MIT Press, first edition, 2001.

[7] Y. Or and E. Rimon. Robust multiple-contact postures in a two-dimensional gravitational field. Technical report, Technion University Dept. of Mechanical Engineering, 2003.

[8] J.S. Pang and J.C. Trinkle. Stability characterizations of rigid body contact problems with coulomb friction. In *Proc. IEEE Int. Conf. on Robotics and Automation*, 2000.

[9] F. Pfeiffer and Christoph Glocker. *Multibody Dynamics with Unilateral Contacts*. Wiley, first edition, 1996.

[10] David E. Stewart. Rigid-body dynamics with friction and impact. *SIAM Review*, 42(1):3–39, 2000.

[11] M. Yim, S. Homans, and K. Roufas. Climbing with snake-like robots. In *Proc. of IFAC Workshop on Mobile Robot Technology*, 2001.